

Scientific Inquiry and Review (SIR)

Volume 7 Issue 4, 2023

ISSN (P): 2521-2427, ISSN (E): 2521-2435

Homepage: <https://journals.umt.edu.pk/index.php/SIR>



Article QR



Title: Plant-Extract of *Mimusops elengi* leaves and Flower-Mediated ZnO Nanoparticles: Synthesis, Characterization, and Biomedical Applications

Author (s): Iram Bashir, Syeda Shaista Gillani*, and Fouzia Majeed

Affiliation (s): Department of Chemistry, Lahore Garrison University, Pakistan

DOI: <https://doi.org/10.32350/sir.74.01>

History: Received: May 31, 2023, Revised: September 11, 2023, Accepted: September 12, 2023, Published: 27 October, 2023

Citation: Bashir I, Gillani SS, Majeed F. Plant-Extract of *Mimusops elengi* leaves and Flower-Mediated ZnO Nanoparticles: Synthesis, Characterization, and Biomedical Applications. *Sci Inq Rev.* 2023;7(4):1–18. <https://doi.org/10.32350/sir.74.01>

Copyright: © The Authors

Licensing:  This article is open access and is distributed under the terms of [Creative Commons Attribution 4.0 International License](https://creativecommons.org/licenses/by/4.0/)

Conflict of Interest: Author(s) declared no conflict of interest



A publication of
The School of Science
University of Management and Technology, Lahore, Pakistan

Plant-Extract of *Mimusops elengi* leaves and Flower-Mediated ZnO Nanoparticles: Synthesis, Characterization, and Biomedical Applications

Iram Bashir, Syeda Shaista Gillani*, and Fouzia Majeed

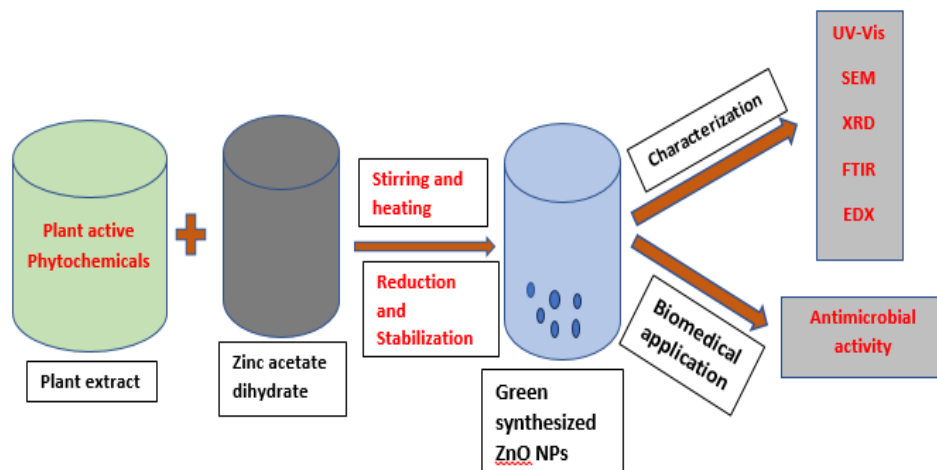
Department of Chemistry, Lahore Garrison University, Pakistan

ABSTRACT

The current study aims to employ an ecologically sustainable method, utilizing a plant-based extract derived from *Mimusops elengi* as both a reducing and capping agent. Synthesis of zinc oxide nanoparticles (ZnO NPs) was done from aqueous leaves and flower extracts of *Mimusops elengi*. Different spectroscopic techniques were used to characterize these biosynthesized (ZnO NPs) zinc oxide nanoparticles like UV-visible, FTIR, XRD, SEM, and EDX techniques. UV-visible spectroscopy showed the absorption wavelength of ZnO NPs at 353nm (leaves extracts) and 365nm (flowers extracts). FTIR spectra showed the absorption frequency of different functional groups present in plant extract along with ZnO peak at 637cm^{-1} (leaves extracts) and 643cm^{-1} (flowers extracts). XRD results revealed the hexagonal structure and crystalline nature of biosynthesized ZnO NPs. The average grain size calculated for ZnO NPs of leaves and flower extracts was 10.37 and 15.52nm, respectively. SEM analysis showed a hexagonal shape. EDX confirmed the formation and purity of ZnO NPs by showing an abundant % of zinc and oxygen atoms. The significant bactericidal efficacy of biosynthesized ZnO NPs was found against pathogens *Escherichia coli* and *Staphylococcus aureus*. When compared to ZnO nanoparticles from flower extracts and biosynthesized ZnO nanoparticles from leaf extract exhibited substantial suppression. ZnO-NPs synthesized from leaves and flower extracts of *Mimusops elengi* can be subjugated for biomedical and ecologically sustainable applications.

* Corresponding Author: shaistaaligillani@gmail.com

Graphical Abstract



Keywords: antibacterial, biomedical, green synthesis, *Mimusops elengi*, nanoparticles (NPs)

1. INTRODUCTION

In 1959, at the California Institute of Technology (Caltech), a Nobel Laureate, Richard Feynman presented a notable speech during a conference hosted by the American Physical Society titled: *There's Plenty of Space at the bottom* [1], in which he explored the groundbreaking concept of nanotechnology and the potential for crafting intricate molecular machines with atomic accuracy. Nanotechnology is the atomic-scale manipulation of matter and has applications in various fields. Nanoparticles (NPs) are microscopic particles made up of both organic and inorganic materials [2]. Due to their tiny size (1-100 nm), high energy at the surface, and larger (S/V) surface area to volume ratio, their catalytic capabilities and interaction with other molecules increased, significantly [3].

In the last decade, comprehensive research concerning metal oxide nanoparticles has been emphasized due to their myriad applications in several technology sectors. Zinc Oxide (ZnO NPs) is one of the materials in nature that show great diversity in the structure, of all known materials and is an interesting inorganic material with several advantages in current laser medical, biomedical, and optoelectronic technology [4–7]. ZnO NPs are categorized as a semiconductor in material science because of their covalent and ionic bonds. Due to a large energy band (3.37 MeV) and broad energy

bond (60MeV), ZnO NPs have captivated a lot of consideration because of their high mechanical capabilities and thermal stability at ambient temperature. ZnO NPs are more appealing and effective in current laser medical technology, electronics, and optoelectronic technology because of this significant characteristic [5].



Figure 1. Some Appealing Properties of Zinc Oxide Nanoparticles

Zinc Oxide nanomaterials possess a range of structures, which act as a novel material and have potential uses in a number of nanotechnology sectors. These particles have showed the potential to photo-oxidize and photo-catalyze chemical reactions and biological species, as a result of this ability, they are a key player in cancer therapy [8].

ZnO is one of five chemicals that are classified as "generally regarded as safe". ZnO has been widely utilized in cosmetics, sunscreens, lotions, medication delivery, and bio-imaging due to its bio safe and biocompatible characteristics [3]. ZnO NPs have been explored as an antibacterial and anticancer agent in several other research investigations [7].

Several techniques are reported for the synthesis of nanoparticles, which are classified into three types: Physical (mechanical), chemical, and biological [9]. Green synthesis is a relatively recent phrase that refers to the employment of ecologically sustainable methods for the creation of new products that do not affect the environment. In physical and chemical methods dangerous substances are being absorbed on the surface [10].

As physical and chemical procedures became more expensive day by day, the necessity for biosynthesis of nanoparticles emerged as a new trend. Chemical synthesis processes usually result in dangerous substances being absorbed on the surface, which may have negative consequences in clinical uses [11, 12]. In order to find cost-effective ways to make nanoparticles, scientists turned to microbial enzymes and plant extracts (phytochemicals), which are generally responsible for the reduction of metals into their respective nanoparticles, due to their antioxidant or reducing capabilities. Green synthesis is less expensive, more eco conscious, and simpler for high yield production than chemical or physical synthesis as it does not need the use of high pressure, power, temperature, or dangerous substances.

The current study focused on the leaves and flowers of *Mimusops elengi* Linn. (*M. elengi*), which is a fragrant ornamental tree belonging to the Sapotaceae family. Hindus regard *Mimusops elengi* as a holy plant and a symbol of love and beauty [13]. The bark of *Mimusops elengi* is used as a cooling agent, a cardi tonic, the blossoms are used to treat asthma, and are smoked [14]. The fruit of *Mimusops elengi* is edible; it has astringent properties, is excellent for the teeth and produces flatulence, the seed is used to repair loose teeth and to treat headaches [15]. The phytochemicals present in the aqueous extract of *Mimusops elengi*, functions as an oxidizing, reducing, and stabilizing agent for the biosynthesis of these zinc oxide nanoparticles (ZnO NPs).

2. MATERIALS AND METHOD

Chemicals: Zinc acetate dihydrate [$\text{Zn}(\text{C}_2\text{H}_3\text{O}_2)_2 \cdot 2\text{H}_2\text{O}$] and sodium hydroxide (NaOH) were purchased from Sigma-Aldrich

All of the reagents and solvents used for this research work were of excellent analytical quality and purchased from Sigma-Aldrich. Solvents were refined by distillation before usage. The leaves and flowers of *Mimusops elengi* were collected from Baagh-e-Jinnah, Lahore, Pakistan.

2.1. Aqueous Extraction of Leaves and Flowers of *Mimusops elengi*

Freshly collected leaves and flowers of *Mimusops elengi* were scrupulously washed with water to remove debris on the surface and then rinsed with distilled water. After that, leaves and flowers were shade-dried for a week, weighed (12g), and crushed to a fine powder, separately. Then, the powder of leaves and flowers was mixed and heated with 100 mL distilled water at 20°C for an hour, while swirling constantly with vigorous

stirring, separately. The mixtures were filtered twice, first with muslin cloth and once with Whatman No. 1 filter paper, separately. Dark green extracts (leaves) and pale orange extracts (flowers) were obtained and stored at 4 °C for further processing.

2.2. Preparation of Salt Solution

5.48g of zinc acetate dihydrate was dissolved in 100 mL of distilled water to produce 0.25M zinc acetate dihydrate ($\text{Zn}(\text{C}_2\text{H}_3\text{O}_2)_2 \cdot 2\text{H}_2\text{O}$) solution.

2.3. Green Synthesis of Zinc Oxide Nanoparticles

A 100 mL of 0.25M zinc acetate dihydrate ($\text{Zn}(\text{C}_2\text{H}_3\text{O}_2)_2 \cdot 2\text{H}_2\text{O}$) solution was mixed with 50 mL leaves extract and 50 mL flowers extract in a 250 mL flask, separately. The colour of the mixture changed from dark green to brown for the leaves and pale orange to brown for the flower extracts after 1 hour of incubation at 40°C with continual shaking, suggesting that green manufactured zinc oxide nanoparticles had been generated. Then 0.02 M NaOH was added drop by drop to keep the pH of the solution at 12. As a result, bio-reduced salt sank to the flask's bottom. After that, the sample was washed with distilled water before being exposed to ethanol. The washing procedure was repeated three times to ensure that all contaminants were eliminated. The washed ZnO NPs were then oven-dried for 24 hours at 60°C. The powdered ZnO NPs were then kept for future analysis.

2.4. Antibacterial Assay

The antibacterial activity of biosynthesized ZnO nanoparticles was tested using two bacterium strains. The antibacterial activity was measured using the Agar well diffusion method. The antibacterial activity of biologically produced zinc oxide (ZnO) nanoparticles against gram-positive (*Staphylococcus aureus*) and gram-negative (*Escherichia coli*) bacterial strains was tested. Three wells were made on each agar plate, added 10 µL ZnO NPs, Ciprofloxacin (standard reference), and left it for 24 hours.

3. RESULTS AND DISCUSSION

3.1. Characterization Techniques

UV- Visible Spectroscopy (Ultra-3000), Fourier transforms infrared (FTIR) spectroscopy, X-ray Diffraction (XRD) (Bruker AXS D8), Scanning

Electron Microscopy (SEM) (HITECH-3400-N), and Energy dispersive X-ray (EDX) analysis was used to characterize the synthesized zinc oxide nanoparticles (ZnO NPs).

3.2. UV-Visible

The UV-visible spectra were recorded on an Ultra 3000 UV-Vis spectrophotometer for these green synthesized ZnO NPs. The spectrophotometer was allowed to scan at wavelength ranges from 200-800nm. The λ_{max} at 353 nm (a) and 365 nm (b) [16] depicts the Surface Plasmon Resonance (SPR) phenomena when the ground state non-bonding electrons excited to a higher energy state [17, 18], as a result, a change in colour was noticed from dark green to brown, while the colour of the flower extract changed from pale orange to light brown. The monodispersed character of NPs distribution is confirmed by the strong absorption peaks of ZnO.

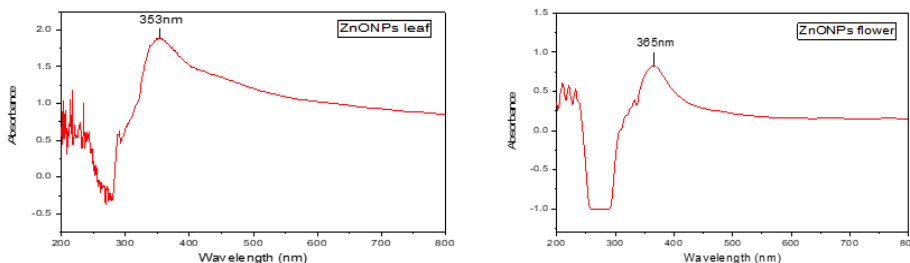


Figure 2. UV-Vis Spectra: (a) Zn ONPs for Leaves Extract and (b) Zn ONPs for Flower Extract

3.2.1. Fourier Transforms Infrared (FTIR). Fourier transforms infrared spectroscopy ($4000\text{--}400\text{ cm}^{-1}$) was used to categorize functional groups in aqueous extract and zinc oxide nanoparticles (ZnO NPs). (FTIR) spectrum of biosynthesized Zn ONPs was used for the leaf extract, which is given in Figure 3. By using the FTIR technique, the phytochemical composition of biomolecules resulted in the reduction and stability of ZnO NPs. The broad peak at 3085cm^{-1} links to the OH [19] group of carboxylic acid along with C=O stretching at 1560cm^{-1} [20]. The peak at 1560cm^{-1} may also be due to the N-H bending of alkaloids or the N=O group showing asymmetric stretching vibrations. The peak at 2313cm^{-1} resulted from =C-H stretch of aromatic aldehyde. The sharp peak at 1408cm^{-1} showed symmetric stretching of the N=O bond or C-N stretch and the peak at

1014 cm^{-1} was because of C-O stretching vibration [21], which represent acidic, alcoholic, phenolic, and aromatic nitro compounds. The fingerprint region of the spectrum contained a peak at 637 cm^{-1} confirming the presence of Zn-O. Previous literature has reported, the range of 400-500 cm^{-1} for the absorption bands [22] or for higher frequencies, however, 608-731 cm^{-1} [23] were indicated for the distinctive peaks for ZnO vibrations.

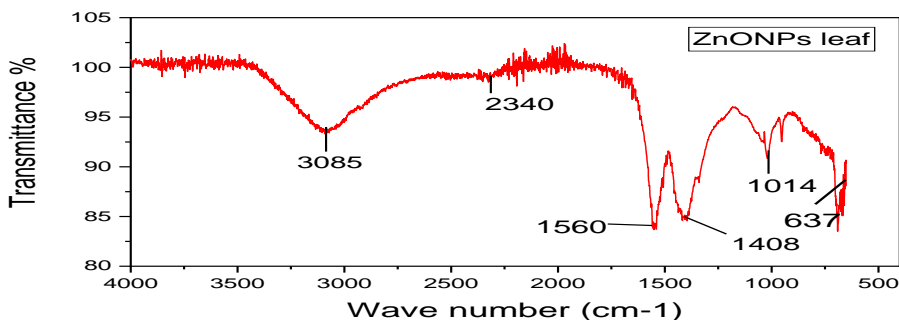


Figure 3. FTIR Spectrum of ZnO NPs (leaves Extract)

Figure 4 shows the IR spectrum of zinc oxide nanoparticles for the flower extract. It showed some characteristic peaks, which were observed because phytochemicals exist in extract and are accountable for nanoparticle fabrication and maintenance. The broad peak at 3120 cm^{-1} was because of the phenolic or alcoholic hydroxyl (OH) group. A small peak at 2880 cm^{-1} resulted from -CH stretching frequency. The high-pitched peak at 1609 cm^{-1} was observed due to carbonyl stretch, aromatic C=C stretching, or N-H bending vibrations. Another sharp peak at 1326 cm^{-1} showed the presence of the C-N group as well as the amide band of proteins [24]. The medium-strong peak at 1103 cm^{-1} links to a stretch of the C-O bond. The signal at 643 cm^{-1} was caused by a Zn-O link, indicating that zinc oxide nanoparticles were synthesized [23].

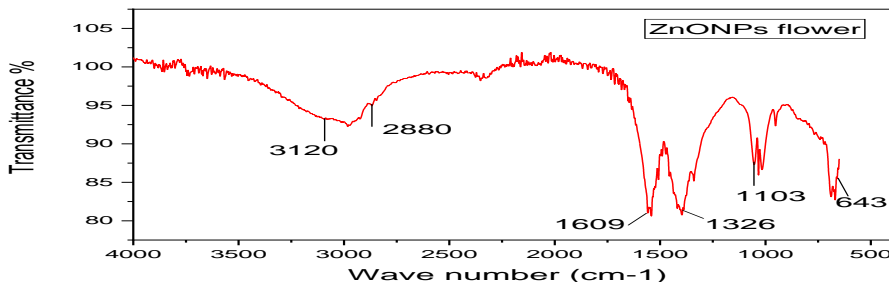


Figure 4. FTIR Spectrum of ZnO NPs (Flowers Extract)

3.2.2. X-ray Diffraction. XRD examination was done to evaluate the crystallographic nature and phase purity of these biosynthesized zinc oxide nanoparticles (see Figure 5). The XRD peaks of ZnO NPs for the leaves extract diffracted at 2θ angle are 31.63° , 34.31° , 37.12° , 47.80° , 57.68° , 63.52° , and 68.84° that showed 100, 002, 101, 102, 110, 103, and 112 Miller indexes planes, respectively. The obtained peaks were consistent with those reported in [25]. The hexagonal wurtzite structure of zinc oxide nanoparticles is represented by all sample's diffraction peaks. Planes of hexagonal ZnO nanoparticles significantly matched with standard card values (JCPDS PDF No 36-1451). The size of the crystalline nanoparticles was enumerated by using the Debye–Scherrer formula [25, 26].

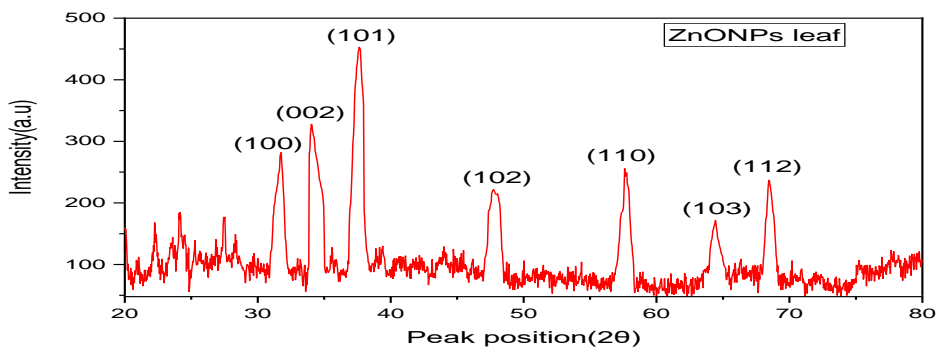


Figure 5. XRD Graph of ZnO NPs (Leaves Extracts)

The X-ray diffraction peaks of green synthesized zinc oxide nanoparticles for the flower extract given in Figure 6 at 2θ diffracted angle are 32.93° , 34.70° , 37.68° , 49.25° , 57.67° , 63.86° , and 69.98° exhibiting 100, 002, 101, 102, 110, 103, and 201 Miller indexes planes, respectively. The Peak search approach was used to compare the peak pattern with the previously reported patterns (found in the library), confirming that the synthesized product has a hexagonal structure due to its distinctive pattern. The crystalline nature of ZnO NPs was revealed by the strong peaks. The single-phase purity of the ZnO NPs is also shown by the placement and sharpness of the peaks [27]. The obtained peaks were consistent with those reported in [25]. The average size calculated was 15.52 nm (Debye Scherrer equation).

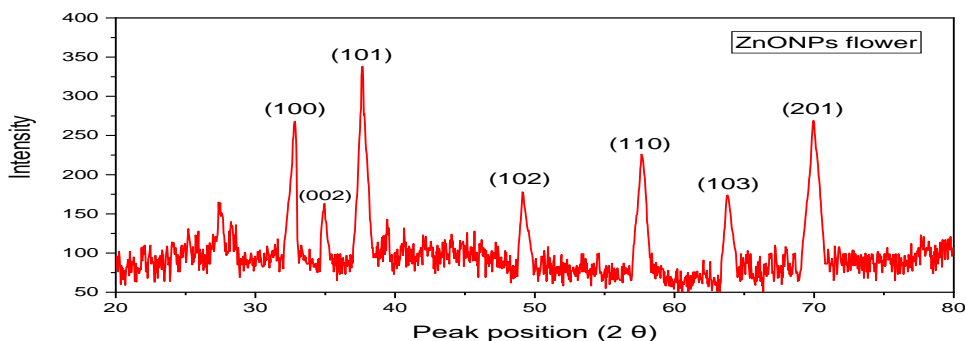


Figure 6. XRD Graph of ZnO NPs (Flowers Extracts)

3.2.3. Scanning Electron Microscopy (SEM). The surface morphology of ZnO NPs from leaves and flower extracts was hexagonal wurtzite (see Figure 7). The average grain size calculated for ZnO NPs of leaves and flower extracts was 10.37 and 15.52nm, respectively. SEM analysis showed a hexagonal shape. Altered forms of ZnO NPs have previously been observed, with sphere-shaped, hexagonal, and flower-like shapes being the most prevalent among them [28, 29].

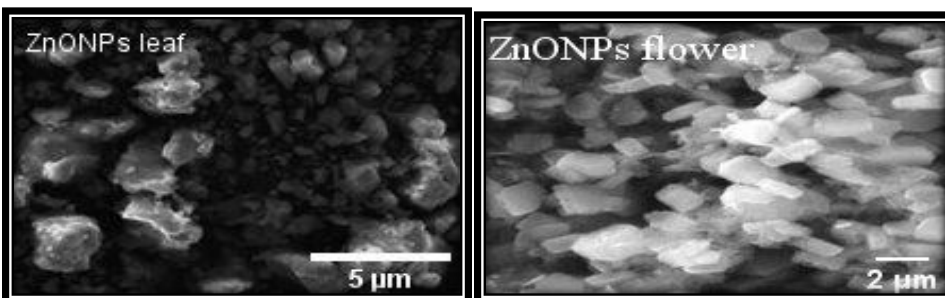


Figure 7. SEM Images of ZnONPs Leaves and Flowers Extracts

3.2.4. Energy Dispersive X-ray (EDX). This technique was utilized to recognize different types of elements present in the selected sample. This study revealed that the current sample contains a significant amount of zinc (52.94% in the leaf and 50.96% in the flower) and oxygen (40.94% in the leaf and 40.08% in the flower) with a trace amount of C, Pb, K, Cl, and P elements. The trace elements may come from the soil and environment of the plant. The elemental distribution of the ZnO NPs was confirmed by the EDX spectra, which indicated the main peaks between 0.5-8.5 keV [30]. The purity of zinc oxide nanoparticles (ZnO NPs) was revealed [31] with high Zn and oxygen element composition and the synthesis of ZnO NPs was

confirmed. The purity of ZnO NPs from the leaf was 93.88% (40.94%+52.94%) and 91.04% (40.08%+50.96%) for the flower ZnO NPs.

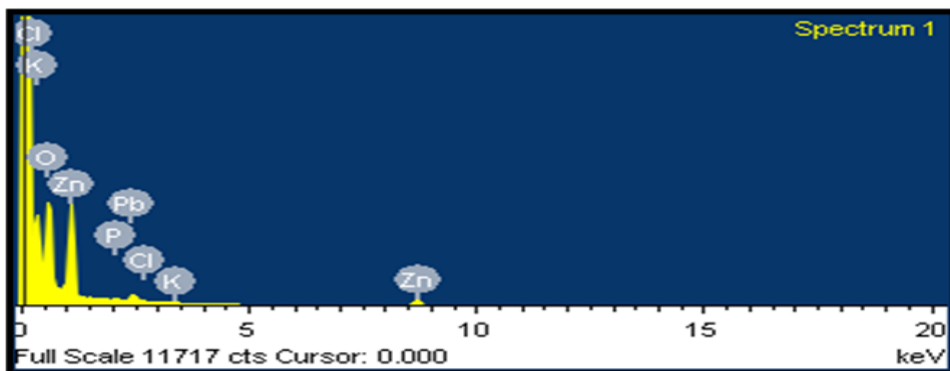


Figure 8. EDX Spectrum of ZnO NPs (Leaves Extracts)

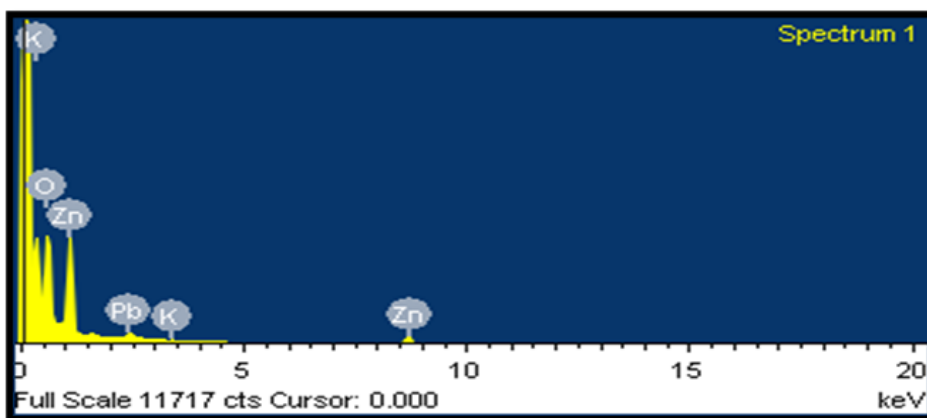


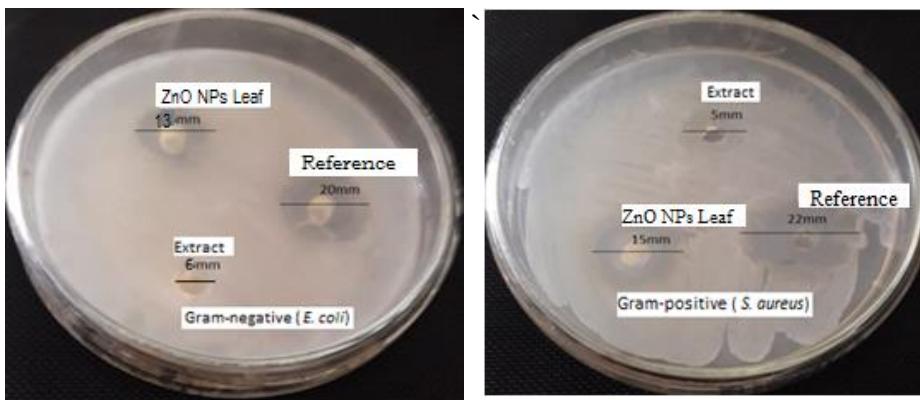
Figure 9. EDX Spectrum of ZnO NPs (Flowers Extracts)

3.3. Measurement of Antibacterial Activity

Biosynthesized zinc oxide nanoparticles from leaves have antibacterial action against pathogens of importance (see Figure 10). The antibacterial activity of ZnO NPs from the leaves at 100 μ g/mL concentration was 13mm, leaves extract showed 6mm, while the reference (Ciprofloxacin) was measured at 20mm zone of inhibition against *E.coli* (Gram-negative) bacteria. Also, *S.aureus* (Gram-positive) bacteria showed 15mm for ZnO NPs, 5mm for leaves, and 22mm zones of inhibition against the reference.

Inhibition zones of zinc oxide nanoparticles (ZnO NPs) produced from *Mimusops elengi* flowers were equally impressive (see Figure 12). Against

E. coli, the ZOI for floral ZnO NPs was 10mm, 15mm for the reference, and 3mm for the flower extract. Additionally, the ZOI against *S. aureus* was measured at 16mm for ZnO NPs 20mm for reference, and 8mm for flowers extract. As the size of ZnO NPs from the leaves is less as compared to ZnO NPs from the flowers, it showed a greater antibacterial effect. Nanoparticles' antibacterial activity is a size-dependent on the characteristics, which gradually improves when the particle size is reduced [32].



Gram-negative *Escherichia coli* Gram-positive *Staphylococcus aureus*

Figure 10. Zone of Inhibitions by Zn ONPs (Leaves Extract)

Table 1. Measured ZOI against *E. coli* and *S. aureus*

Clinical pathogenic strains	ZOI (mm)		
	Leaves extract	ZnO NPs (Leaves extracts)	Reference (Ciprofloxacin)
(a) <i>Escherichia coli</i>	6mm	13mm	20mm
(b) <i>Staphylococcus aureus</i>	5mm	15mm	22mm

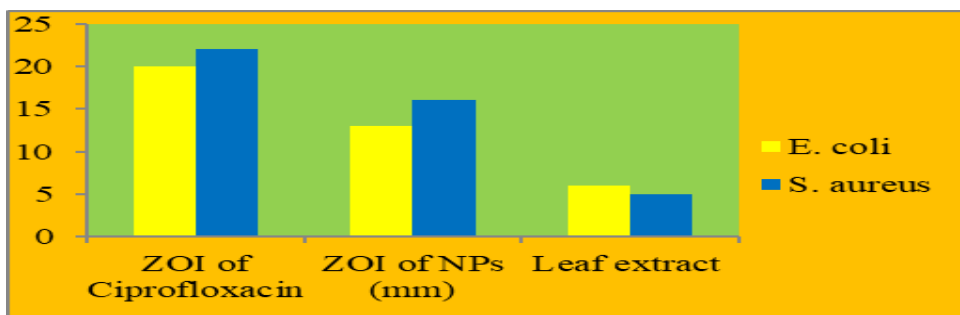
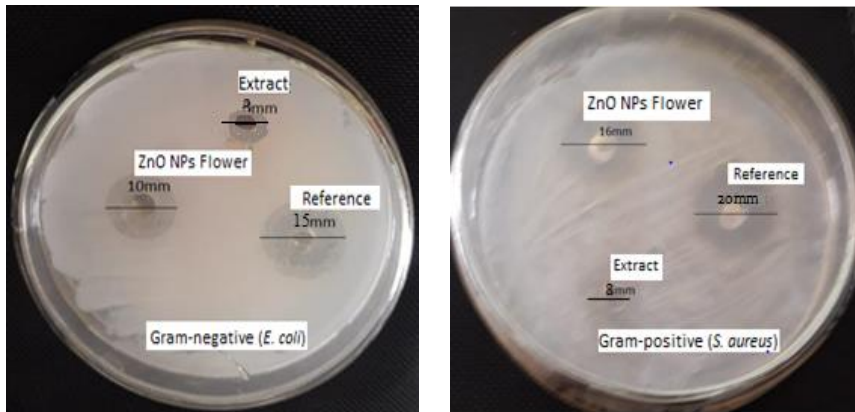


Figure 11. Bar Graph for the Measured Zone of Inhibition



Gram-negative *Escherichia coli* Gram-positive *Staphylococcus aureus*

Figure 12. Zone of Inhibition by ZnO NPs (Flowers Extract)

Table 2. Measured Zones of Inhibition of ZnO NPs from Flower

Clinical pathogenic strains	Zone of Inhibition (ZOI) (mm)		
	Flowers extract	ZnO NPs (Flowers extract)	Reference (Ciprofloxacin)
(a) <i>Escherichia coli</i>	3mm	10 mm	15mm
(b) <i>Staphylococcus aureus</i>	8 mm	16 mm	20mm

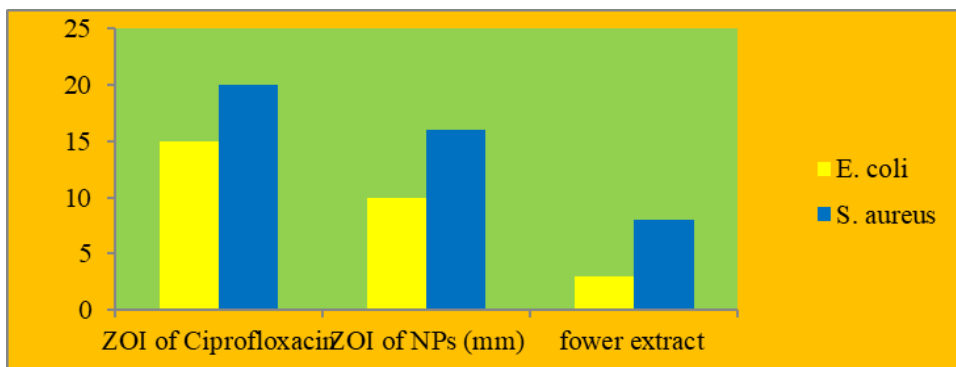


Figure 13. Bar Graph Representing the ZOI against *E. coli* and *S. aureus*

The presence of an inhibitory zone indicates that ZnO nanoparticles' biocidal action involves membrane rupture with a greater rate of surface oxygen species, which results in pathogen loss. ZnO nanoparticles produced from *Mimusops elengi* leaves and flower extract exhibit antibacterial

properties. According to the findings, ZnO nanoparticles were made from *Mimulus elengi* leaf and flower extract against *E.coli* and *S.aureus*. In comparison to ZnO nanoparticles (flowers), biosynthesized ZnO nanoparticles (leaves) exhibited substantial suppression [33].

4. CONCLUSION

Conclusively, this study provided a convenient and cost-effective method to synthesize ZnO NPs by using *Mimulus elengi* as a novel reducing and stabilizing agent. The ZnO NPs were characterized by SEM, UV-Vis, FTIR, XRD, and EDX spectroscopy. UV-visible spectroscopy showed the maxima absorption of ZnO NPs at 353nm (leaves extracts) and 365nm (flowers extracts). FTIR spectra showed the absorption frequency of different functional groups present in plant extract along with ZnO peak at 637cm⁻¹ (leaves extracts) and 643cm⁻¹ (flowers extracts). XRD results revealed the hexagonal structure and crystalline nature of biosynthesized ZnO NPs. The average grain size calculated for ZnO NPs of leaves and flower extracts was 10.37 and 15.52nm, respectively. SEM analysis showed a hexagonal shape. EDX confirmed the formation and purity of ZnO NPs by showing an ample % of zinc and oxygen atoms. ZnO NPs showed significant antibacterial activity against clinical pathogens *Escherichia coli* and *Staphylococcus aureus*. ZnO NPs synthesized from flowers showed a higher bactericidal impact on the tested pathogens in comparison to ZnO NPs synthesized, which was synthesized from leaves. Certainly, green - synthesized zinc oxide nanoparticles (ZnO NPs) were ecologically sustainable, and can be employed in various biological applications.

REFERENCES

1. Treguer M, De Cointet C, Remita H, et al. Dose rate effects on radiolytic synthesis of gold- silver bimetallic clusters in solution. *J Phys Chem.* 1998;102(22):4310–4321. <https://doi.org/10.1021/jp981467n>
2. LaConte L, Nitin N, Bao G. Magnetic nanoparticle probes. *Mater Today.* 2005;8(5):32–38. [https://doi.org/10.1016/S1369-7021\(05\)00893-X](https://doi.org/10.1016/S1369-7021(05)00893-X)
3. Iqbal J, Abbasi BA, Mahmood T, Hameed S, Munir A, Kanwal S. Green synthesis and characterizations of Nickel oxide nanoparticles using leaf extract of *Rhamnus virgata* and their potential biological applications. *Appl Organomet Chem.* 2019;33(8):e4950. <https://doi.org/10.1002/aoc.4950>

4. Altavilla C, Ciliberto E. *Inorganic Nanoparticles: Synthesis, Applications, and Perspectives*. CRC Press; 2017.
5. Wang J, Cao J, Fang B, Lu P, Deng S, Wang H. Synthesis and characterization of multipod, flower-like, and shuttle-like ZnO frameworks in ionic liquids. *Mat Lett*. 2005;59(11):1405–1408. <https://doi.org/10.1016/j.matlet.2004.11.062>
6. Bacaksiz E, Parlak M, Tomakin M, Özçelik A, Karakız M, Altunbaş M. The effects of zinc nitrate, zinc acetate and zinc chloride precursors on investigation of structural and optical properties of ZnO thin films. *J Alloys Comp*. 2008;466(1-2):447–450. <https://doi.org/10.1016/j.jallcom.2007.11.061>
7. Abbasi BA, Iqbal J, Mahmood T, Qyyum A, Kanwal S. Biofabrication of iron oxide nanoparticles by leaf extract of *Rhamnus virgata*: characterization and evaluation of cytotoxic, antimicrobial and antioxidant potentials. *Appl Organomet Chem*. 2019;33(7):e4947. <https://doi.org/10.1002/aoc.4947>
8. Zhang H, Chen B, Jiang H, Wang C, Wang H, Wang X. A strategy for ZnO nanorod mediated multi-mode cancer treatment. *Biomaterials*. 2011;32(7):1906–1914. <https://doi.org/10.1016/j.biomaterials.2010.11.027>
9. Iravani S, Korbekandi H, Mirmohammadi SV, Zolfaghari B. Synthesis of silver nanoparticles: chemical, physical and biological methods. *Res Pharm Sci*. 2014;9(6):385–406.
10. De Melo CG, Pereira LHDS, Da Costa LAG, et al. Experimental methodologies for the obtainment of *Momordica charantia* L. extracts with anthelmintic activity: a review. *Pharmaco Rev*. 2022;16(32):82–89.
11. Kumar DS, Xavier TF. Antibacterial activity, biosynthesis and characterization of silver nanoparticle from the leaf extract of (*L.*) Nees. *andrographis echioides*. *Asian J Pharm Pharmacol*. 2019;5(1):95–100. <https://doi.org/10.31024/ajpp.2019.5.1.14>
12. Begum NA, Mondal S, Basu S, Laskar RA, Mandal D. Biogenic synthesis of Au and Ag nanoparticles using aqueous solutions of Black Tea leaf extracts. *Colloids Surf B*. 2009;71(1):113–118. <https://doi.org/10.1016/j.colsurfb.2009.01.012>

13. Kadam PV, Yadav KN, Deoda RS, Shivatare RS, Patil MJ. *Mimusops elengi*: a review on ethnobotany, phytochemical and pharmacological profile. *J Pharmaco Phytochem.* 2012;1(3):64–74.
14. Zahid H, Rizwani GH, Shareef H, Mahmud S, Ali T. Hypoglycemic and hypolipidemic effects of *Mimusops elengi* Linn, extracts on normoglycaemic and alloxaninduced diabetic rats. *Int J Pharmal Biol Arch.* 2012;3(1):56–62.
15. Gami B, Pathak S, Parabia M. Ethnobotanical, phytochemical and pharmacological review of *Mimusops elengi* Linn. *Asian Pa J Trop Biomed.* 2012;2(9):743–748. [https://doi.org/10.1016/S2221-1691\(12\)60221-4](https://doi.org/10.1016/S2221-1691(12)60221-4)
16. Nagajyothi P, Sreekanth T, Tettey CO, Jun YI, Mook SH. Characterization, antibacterial, antioxidant, and cytotoxic activities of ZnO nanoparticles using *Coptidis Rhizoma*. *Bioorg Med Chem Lett.* 2014;24(17):4298–4303. <https://doi.org/10.1016/j.bmcl.2014.07.023>
17. Gurgur E, Oluyamo S, Adetuyi A, Omotunde O, Okoronkwo A. Green synthesis of zinc oxide nanoparticles and zinc oxide–silver, zinc oxide–copper nanocomposites using *Bridelia ferruginea* as biotemplate. *SN Appl Sci.* 2020;2:1–12. <https://doi.org/10.1007/s42452-020-2269-3>
18. Talam S, Karumuri SR, Gunnam N. Synthesis, characterization, and spectroscopic properties of ZnO nanoparticles. *Int Scholar Res Not.* 2012;2012:e372505. <https://doi.org/10.5402/2012/372505>
19. Vijayalakshmi U, Chellappa M, Anjaneyulu U, Manivasagam G, Sethu S. Influence of coating parameter and sintering atmosphere on the corrosion resistance behavior of electrophoretically deposited composite coatings. *Mat Manufac Proc.* 2016;31(1):95–106. <https://doi.org/10.1080/10426914.2015.1070424>
20. Stan M, Popa A, Toloman D, Silipas T-D, Vodnar DC. Antibacterial and antioxidant activities of ZnO nanoparticles synthesized using extracts of *Allium sativum*, *Rosmarinus officinalis* and *Ocimum basilicum*. *Acta Metallur Sinica.* 2016;29:228–236. <https://doi.org/10.1007/s40195-016-0380-7>
21. Huang J, Li Q, Sun D, et al. Biosynthesis of silver and gold nanoparticles by novel sundried *Cinnamomum camphora* leaf.

- Nanotechnology*. 2007;18(10):e105104. <https://doi.org/10.1088/0957-4484/18/10/105104>
22. Shamhari NM, Wee BS, Chin SF, Kok KY. Synthesis and characterization of zinc oxide nanoparticles with small particle size distribution. *Acta Chim Sloven*. 2018;65(3):578–585. <https://doi.org/10.17344/acsi.2018.4213>
 23. Jayarambabu N, Kumari BS, Rao KV, Prabhu Y. Beneficial role of zinc oxide nanoparticles on green crop production. *Int J Multidiscip Adv Res Trends*. 2015;2:273–282.
 24. Jain N, Bhargava A, Majumdar S, Tarafdar J, Panwar J. Extracellular biosynthesis and characterization of silver nanoparticles using *Aspergillus flavus* NJP08: a mechanism perspective. *Nanoscale*. 2011;3(2):635–641. <https://doi.org/10.1039/C0NR00656D>
 25. Barzinjy AA, Azeez HH. Green synthesis and characterization of zinc oxide nanoparticles using *Eucalyptus globulus* Labill. leaf extract and zinc nitrate hexahydrate salt. *SN Appl Scis*. 2020;2(5):e991. <https://doi.org/10.1007/s42452-020-2813-1>
 26. Muhammad W, Ullah N, Haroon M, Abbasi BH. Optical, morphological and biological analysis of zinc oxide nanoparticles (ZnO NPs) using *Papaver somniferum* L. *RSC Adv*. 2019;9(51):29541–29548. <https://doi.org/10.1039/C9RA04424H>
 27. Khatami M, Alijani HQ, Heli H, Sharifi I. Rectangular shaped zinc oxide nanoparticles: green synthesis by *Stevia* and its biomedical efficiency. *Ceram Int*. 2018;44(13):15596–15602. <https://doi.org/10.1016/j.ceramint.2018.05.224>
 28. Khan MA, Abbasi BH, Shinwari ZK. Thidiazuron enhanced regeneration and silymarin content in *Silybum marianum* L. *Pak J Bot*. 2014;46(1):185–190.
 29. Ramesh M, Anbuvaran M, Viruthagiri G. Green synthesis of ZnO nanoparticles using *Solanum nigrum* leaf extract and their antibacterial activity. *Spectrochim Acta A Mol Biomol Spectrosc*. 2015;136:864–870. <https://doi.org/10.1016/j.saa.2014.09.105>

30. Kumar SS, Venkateswarlu P, Rao VR, Rao GN. Synthesis, characterization and optical properties of zinc oxide nanoparticles. *Int Nano Lett.* 2013;3:e30. <https://doi.org/10.1186/2228-5326-3-30>
31. Fakhari S, Jamzad M, Fard HK. Green synthesis of zinc oxide nanoparticles: a comparison. *Green Chem Lett Rev.* 2019;12(1):19–24. <https://doi.org/10.1080/17518253.2018.1547925>
32. Raghupathi KR, Koodali RT, Manna AC. Size-dependent bacterial growth inhibition and mechanism of antibacterial activity of zinc oxide nanoparticles. *Langmuir.* 2011;27(7):4020–4028. <https://doi.org/10.1021/la104825u>
33. Ratney YJJ, David SB. Antibacterial activity of zinc oxide nanoparticles by sonochemical method and green method using *Zingiber officinale*. *Green Chem Tech Lett.* 2016;2:11–15. <https://doi.org/10.18510/gctl.2016.212>